PHYSICAL REVIEW B **75**, 161103(R) (2007)

Retardation effects in the Holstein-Hubbard chain at half filling

Ka-Ming Tam,[1] S.-W. Tsai,[2] D. K. Campbell,[1] and A. H. Castro Neto[1]
[1]*Department of Physics, Boston University, 590 Commonwealth Avenue, Boston, Massachusetts 02215, USA*
[2]*Department of Physics, University of California, Riverside, California 92508, USA*
(Received 28 March 2007; published 18 April 2007)

The ground-state phase diagram of the half filled one-dimensional Holstein-Hubbard model contains a charge-density-wave (CDW) phase, driven by the electron-phonon (*e-ph*) coupling, and a spin-density-wave (SDW) phase, driven by the on-site electron-electron (*e-e*) repulsion. Recently, the existence of a third phase, which is metallic and lies in a finite region of parameter space between these two gapped phases, has been claimed. We study this claim using a renormalization-group method for interacting electrons that has been extended to include also *e-ph* couplings. Our method [Tsai *et al.*, Phys. Rev. B **72**, 054531 (2005); Philos. Mag. B **86**, 2631 (2006)] treats *e-e* and *e-ph* interactions on an equal footing and takes retardation effects fully into account. We find a direct transition between the SDW and CDW states. We study the effects of retardation, which are particularly important near the transition, and find that umklapp processes *at finite frequencies* drive the CDW instability close to the transition.

DOI: 10.1103/PhysRevB.75.161103 PACS number(s): 71.10.Fd, 71.30.+h, 71.45.Lr

The interplay between electron-electron (*e-e*) and electron-phonon (*e-ph*) interactions leads to important effects in low-dimensional materials such as molecular crystals, charge transfer solids,[2] conducting polymers,[3] and fullerenes.[4] In narrow-band electronic materials, perhaps the simplest model capturing this interplay is the Holstein-Hubbard model (HHM), where the *e-e* interactions are described by an on-site repulsive Coulomb term, and the electrons are coupled to dispersionless optical phonons in localized vibrational modes.[5]

In the one-dimensional HHM (1DHHM) at half filling, early quantum Monte Carlo (QMC) calculations[6] suggested that there are only two phases: the Peierls charge-density-wave (CDW) and the Mott spin-density-wave (SDW) states.[7] The boundary between these two phases was predicted to lie along the line in parameter space where an "effective" *e-e* interaction vanishes: $U_{\mathrm{eff}}=U-2g_{\mathrm{ep}}^2/\omega_0\simeq 0$, where U is the Hubbard on-site *e-e* repulsion, g_{ep} is the electron-phonon coupling, and ω_0 is the phonon frequency. More recently, several authors have proposed that a third phase might exist near $U_{\mathrm{eff}}\simeq 0$: a metallic, Luttinger liquid, phase,[8–10] or an off-site pairing superconducting phase.[11] Large scale QMC studies[12] have indicated that there is a metallic region with dominant superconducting (SC) pairing correlations between the CDW and SDW regions. Density-matrix renormalization group (DMRG) studies[13] suggest that SC does not exist but instead that both the spin and charge gaps vanish only for $U_{\mathrm{eff}}\simeq 0$, suggesting that a metallic phase (with no dominant SC correlations) may exist only exactly on the boundary between the CDW and SDW phases. This is also the conclusion of two-step renormalization-group studies[15] and Lanczos diagonalization.[14] To attempt to determine which of these scenarios is correct, we study the problem here using a recently developed extended renormalization-group approach.[1].

At half filling, umklapp scattering creates a strong tendency to open a charge gap. From the perspective of weak-coupling approaches, it is highly nontrivial to have a finite metallic, or SC, region. If such a phase is to exist, it must be that the dynamical nature of the phonons effectively suppresses umklapp scattering. Therefore retardation effects must be taken into account in order to investigate this issue. For this purpose, we use a multiscale functional renormalization-group (MFRG) method.[1] Our MFRG is an extension of the RG for interacting fermions[16] that are also coupled to bosonic modes and applies to both the weak ($\lambda \ll 1$) and strong ($\lambda \gg 1$) electron-phonon coupling limit [$\lambda=2N(0)g_{\mathrm{ep}}^2/\omega_0$, $N(0)$ is the electron density of states at the Fermi level]. For a spherical Fermi surface, the MFRG reproduces Eliashberg's theory at the SC instability,[1] and it has been applied in the study of phonons in ladder systems.[17]

The 1DHHM is given by the Hamiltonian

$$H=-t\sum_{i,\sigma}(c_{i+1,\sigma}^{\dagger}c_{i,\sigma}+\mathrm{H.c.})+U\sum_{i}n_{i,\uparrow}n_{i,\downarrow}+g_{\mathrm{ep}}\sum_{i,\sigma}(a_i^{\dagger}+a_i)n_{i,\sigma}+\omega_0\sum_{i}a_i^{\dagger}a_i, \tag{1}$$

where $c_{i,\sigma}^{\dagger}$ ($c_{i,\sigma}$) is an electron creation (annihilation) operator at site i with spin σ, $n_{i\sigma}$ is the electron number operator, $a_i^{\dagger}$ (a_i) is a creation (annihilation) operator for an optical phonon at site i, t is the nearest-neighbor electron hopping integral. We use units such that $t=1=\hbar$.

Using path-integral formulation and integrating the phonon fields, the effective retarded *e-e* interaction is[1]

$$g(\underline{k}_1,\underline{k}_2,\underline{k}_3,\underline{k}_4)=U-\frac{2g_{\mathrm{ep}}^2\omega_0}{[\omega_0^2+(\omega_1-\omega_4)^2]}, \tag{2}$$

where $\underline{k}=(k,\omega)$.[18] We use a notation in which, after scattering, an incoming electron with momentum and frequency $\underline{k}_1$ ($\underline{k}_2$) goes out with $\underline{k}_4$ ($\underline{k}_3$), so that $\underline{k}_1+\underline{k}_2=\underline{k}_3+\underline{k}_4$. In the antiadiabatic limit, where $\omega_0\to\infty$, all the electronic frequency dependences are suppressed, and the HHM maps onto the standard Hubbard model with a renormalized U_{eff}. At half

filling, its ground state is charge-gapped SDW for repulsive interactions and spin-gapped degenerate CDW/SC for attractive interactions. The transition between SDW and degenerate CDW/SC occurs when the bare coupling changes sign ($U_{\text{eff}}=0$).

In the MFRG approach at the one-loop level, the RG flow equations for the coupling *functions*, $g(\underline{k}_1,\underline{k}_2,\underline{k}_3,\underline{k}_4)$ with initial conditions given by Eq. (2), are given by[1]

$$\frac{dg(\underline{k}_1,\underline{k}_2,\underline{k}_3)}{d\Lambda} = -\int d\underline{p}\frac{d}{d\Lambda}[G_\Lambda(\underline{p})G_\Lambda(\underline{k})]g(\underline{k}_1,\underline{k}_2,\underline{k})g(\underline{p},\underline{k},\underline{k}_3) - \int d\underline{p}\frac{d}{d\Lambda}[G_\Lambda(\underline{p})G_\Lambda(\underline{q}_1)]g(\underline{p},\underline{k}_2,\underline{q}_1)g(\underline{k}_1,\underline{q}_1,\underline{k}_3)$$
$$-\int d\underline{p}\frac{d}{d\Lambda}[G_\Lambda(\underline{p})G_\Lambda(\underline{q}_2)][-2g(\underline{k}_1,\underline{p},\underline{q}_2)g(\underline{q}_2,\underline{k}_2,\underline{k}_3)+g(\underline{p},\underline{k}_1,\underline{q}_2)g(\underline{q}_2,\underline{k}_2,\underline{k}_3)+g(\underline{k}_1,\underline{p},\underline{q}_2)g(\underline{k}_2,\underline{q}_2,\underline{k}_3)], \quad (3)$$

where $\underline{k}=\underline{k}_1+\underline{k}_2-\underline{p}$, $\underline{q}_1=\underline{p}+\underline{k}_3-\underline{k}_1$, $\underline{q}_2=\underline{p}+\underline{k}_3-\underline{k}_2$, $\int d\underline{p}=\int dp\Sigma_\omega 1/(2\pi\beta)$, and G_Λ is the self-energy corrected propagator at energy cutoff Λ. Since the interaction vertices are frequency dependent, there are also self-energy corrections. At the one-loop level

$$\frac{d\Sigma(\underline{k})}{d\Lambda} = -\int d\underline{p}\frac{d}{d\Lambda}[G_\Lambda(\underline{p})][2g(\underline{p},\underline{k},\underline{k})-g(\underline{k},\underline{p},\underline{k})]. \quad (4)$$

We have solved the coupled integral-differential equations, Eqs. (3) and (4), numerically with two Fermi points ($N_k=2$) and by dividing the frequency axis into 15 segments ($N_\omega=15$). Figure 1 shows the discretization scheme for $N_k=2$ and $N_\omega=15$.

We next calculate within our MFRG approach the RG flow of susceptibilities in the static (zero frequency) and long-wavelength limit. The SC susceptibility is $\chi_\Lambda^{\text{SC}}(0,0)=\int D(1,2)\langle c_{p_1,\downarrow}c_{-p_1,\uparrow}c^\dagger_{-p_2,\uparrow}c^\dagger_{p_2,\downarrow}\rangle$; and the SDW and CDW susceptibilities can be written as

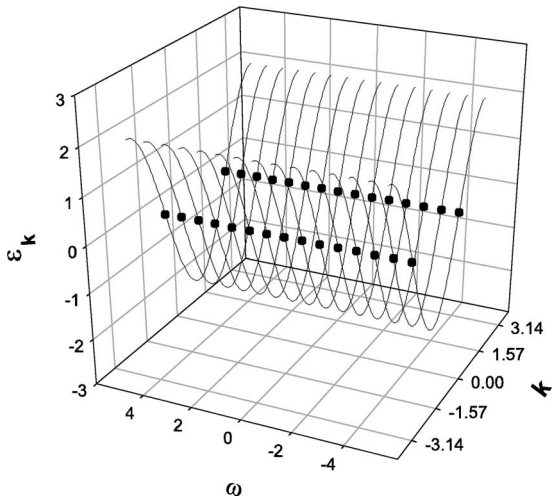

FIG. 1. Discretization of the momenta in the Brillouin zone and frequencies in the frequencies axis. This figure shows the case $N_k=2$, $N_w=15$.

$$\chi_\Lambda^\delta(\pi,0) = \int D(1,2)\langle c^\dagger_{p_1,\sigma_1}c_{p_1+\pi,\sigma_1}c^\dagger_{p_2+\pi,\sigma_2}c_{p_2,\sigma_2}\rangle,$$

where p_i is the momentum at energy ξ_i,

$$\int D(1,2) \equiv \int_{|\xi_1|>\Lambda} d\xi_1 J(\xi_1)\int_{|\xi_2|>\Lambda} d\xi_2 J(\xi_2)\sum\nolimits_{\sigma_1,\sigma_2} s_{\sigma_1}s_{\sigma_2},$$

and $J(\xi)$ is the Jacobian for the coordinate transformation from k to ξ_k. For δ=SDW, $s_\uparrow=1$, $s_\downarrow=-1$, and for δ=CDW, $s_\uparrow=1$, $s_\downarrow=1$. The dominant instability is determined by the most divergent susceptibility as the cutoff Λ is lowered. The flow for the SC susceptibility is given by

$$\frac{d\chi_\Lambda^{\text{SC}}(0,0)}{d\Lambda} = \int d\underline{p}\frac{d}{d\Lambda}[G_\Lambda(\underline{p})G_\Lambda(-\underline{p})][Z_\Lambda^{\text{SC}}(\underline{p})]^2, \quad (5)$$

$$\frac{dZ_\Lambda^{\text{SC}}(\underline{p})}{d\Lambda} = -\int d\underline{p}'\frac{d}{d\Lambda}[G_\Lambda(\underline{p}')G_\Lambda(-\underline{p}')]Z_\Lambda^{\text{SC}}(\underline{p}')g^{\text{SC}}(\underline{p}',\underline{p}), \quad (6)$$

where $g^{\text{SC}}(\underline{p}',\underline{p})=g(\underline{p}',-\underline{p}',-\underline{p})$, and the flows for the SDW and CDW susceptibilities are

$$\frac{d\chi_\Lambda^\delta(\pi,0)}{d\Lambda} = -\int d\underline{p}\frac{d}{d\Lambda}[G_\Lambda(\underline{p})G_\Lambda(\underline{p}+\underline{Q})][Z_\Lambda^\delta(\underline{p})]^2, \quad (7)$$

$$\frac{dZ_\Lambda^\delta(\underline{p})}{d\Lambda} = \int d\underline{p}'\frac{d}{d\Lambda}[G_\Lambda(\underline{p}')G_\Lambda(\underline{p}'+\underline{Q})]Z_\Lambda^\delta(\underline{p}')g^\delta(\underline{p}',\underline{p}), \quad (8)$$

where $\underline{Q}=(\pi,0)$. For δ=SDW, $g^\delta(\underline{p}',\underline{p})=-g(\underline{p}+\underline{Q},\underline{p}',\underline{p})$, and for δ=CDW, $g^\delta(\underline{p}',\underline{p})=2g(\underline{p}',\underline{p}+\underline{Q},\underline{p})-g(\underline{p}+\underline{Q},\underline{p}',\underline{p})$.The function $Z^\delta(\underline{p})$ is the effective vertex in the definition of the susceptibility χ^δ. Its initial RG value is 1. The MFRG equations for susceptibilities are solved with initial condition $\chi^\delta_{\Lambda=\Lambda_0}=0$.

In g-ology[19–21] there are only four couplings, corresponding to forward (g_2,g_4), backward (g_1), and umklapp (g_3) scattering. The charge and the spin parts are governed by g_3 and g_1, respectively. Under the MFRG, each one of these couplings carries frequency dependence $g_i(\omega_1,\omega_2,\omega_3)$. In the

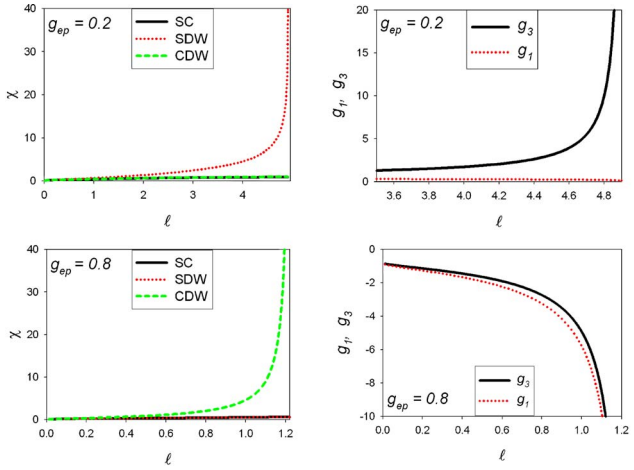

FIG. 2. (Color online) Left: flows of SC, SDW, and CDW susceptibilities for $U=0.5$ and $\omega_0=1.0$. Right: flows of umklapp g_3 and backscattering g_1 at zero frequencies. Top: $g_{ep}=0.2$ ($U_{\text{eff}}>0$). Bottom: $g_{ep}=0.8$ ($U_{\text{eff}}<0$).

weak *e-ph* coupling limit ($\lambda \ll 1$), the two-step RG is a good approximation, and the couplings are separated into two types: high-frequency transfer, $|\omega_1-\omega_4|>\omega_0$, and low-frequency transfer, $|\omega_1-\omega_4|<\omega_0$. However, our MFRG analysis reveals that the couplings develop additional nontrivial frequency dependence, particularly when the *e-ph* coupling is comparable to the *e-e* coupling and $U_{\text{eff}}\approx 0$. As we shall see, understanding this frequency structure is critical to resolving the current controversy about the behavior in the region near the CDW-SDW transition.

Deep inside the CDW and SDW regions, we fix $\omega_0=1.0$ and $U=0.5$, and show results of the RG flows for the susceptibilities and couplings for different values of g_{ep}. For small *e-ph* coupling ($g_{\text{ep}}=0.2$, and $U_{\text{eff}}>0$), the SDW susceptibility exhibits a strong divergence, while both CDW and SC susceptibilities are suppressed (Fig. 2, top). This is expected, since the on-site repulsion dominates over the retarded attractive interaction mediated by the phonons. A charge gap develops, with no spin gap, which can be inferred from the flow of the couplings: umklapp (g_3) diverges, whereas backscattering (g_1) does not. For large *e-ph* coupling ($g_{\text{ep}}=0.8$ and $U_{\text{eff}}<0$), the CDW susceptibility diverges (Fig. 2, bottom). Now there are both spin and charge gaps, and, correspondingly, both umklapp (g_3) and backscattering (g_1) are divergent.

We next consider the region close to the CDW-SDW transition where $U_{\text{eff}}\simeq 0$. For U_{eff} slightly below zero ($g_{\text{ep}}=0.48$), the behavior of susceptibilities and couplings is qualitatively the same as in the rest of the SDW phase (Fig. 2, top). The only difference is that the gap decreases and eventually goes to zero at the transition. Figure 3 shows the flows for $g_{\text{ep}}=0.55$ (U_{eff} slightly above zero). The SC susceptibility becomes enhanced, but the CDW susceptibility still dominates. Interestingly, $g_1(0,0,0)$ diverges but $g_3(0,0,0)$ does not. In 1D problems without retardation, the usual interpretation is that the CDW instability occurs when $g_1\to-\infty$ and $g_3\to-\infty$.[19,21,22] In the present case, since $g_3(0,0,0)\to 0$, we need to look at the frequency dependence of the couplings in order to understand what is driving the CDW instability.

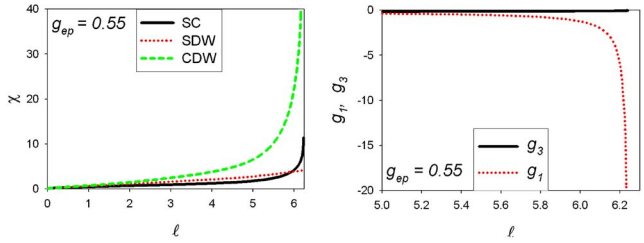

FIG. 3. (Color online) Left: flow of susceptibilities for $U=0.5$, $\omega_0=1.0$, $g_{\text{ep}}=0.55$ ($U_{\text{eff}}<0$). Right: flows of the umklapp scattering g_3 and backscattering g_1 at zero frequency.

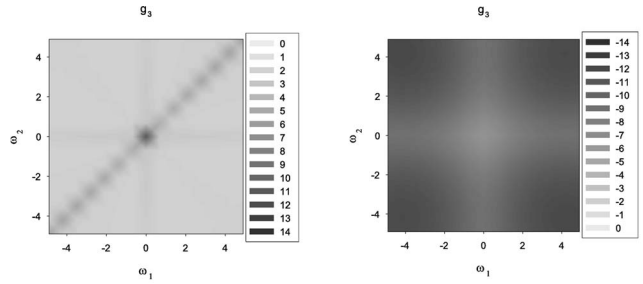

FIG. 4. Plots of the umklapp scattering $g_3(\omega_1,\omega_2,\omega_2,\omega_1)$ for $U=0.5$ and $\omega_0=1.0$. Left: $g_{\text{ep}}=0.2$. Right: $g_{\text{ep}}=0.8$.

In the MFRG approach, we obtain the flows of all the $g_i(\omega_1,\omega_2,\omega_3)$ couplings and self-energies, and can analyze how this frequency dependence evolves with the flow. Consider first the cases deep in the SDW and CDW phases. Figure 4 shows contour plots of $g_3(\omega_1,\omega_2,\omega_2,\omega_1)$ which corresponds to an umklapp process with zero-frequency transfer, $|\omega_1-\omega_4|=0$. We plot the value of the coupling at an RG scale ℓ right before the critical scale ℓ_c when the instability occurs. For the SDW phase (Fig. 4, left), the existence of a charge gap is signaled by divergence in the umklapp channel, and the most divergent g_3 couplings are the ones close to zero frequency. Deep inside the CDW phase, $g_3(0,0,0,0)$

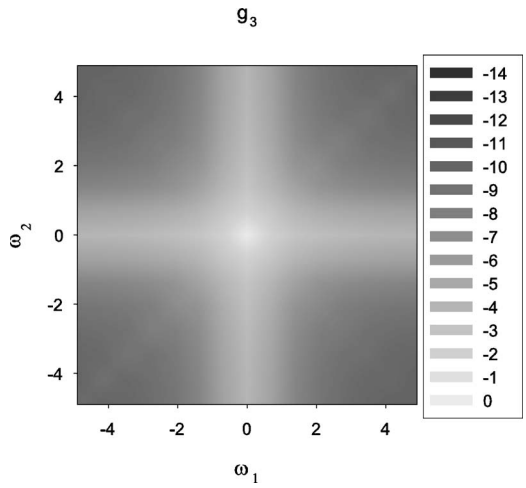

FIG. 5. Plot of the umklapp scattering $g_3(\omega_1,\omega_2,\omega_2,\omega_1)$ for $U=0.5$, $\omega_0=1.0$, and $g_3=0.55$. Note that $g_3(0,0,0,0)$ is flowing towards zero.

also diverges, as seen before (Fig. 2). However, the most divergent couplings are for large values of ω_1 and ω_2 (Fig. 4).

The situation for $g_{ep}=0.55$, shown in Fig. 5, is more intriguing. Umklapp scattering is renormalized to large values in most parts of the frequency space. However, for frequencies near zero umklapp scattering flows to very small values. From the RG flow of the susceptibilities (Figs. 2 and 3), it is clear that there is CDW instability for $U_{\text{eff}}>0$ and a direct transition from CDW to SDW. From the frequency dependence of g_3 we conclude that close to the transition to the SDW, the CDW instability is being driven by umklapp processes *at high frequencies*. These are processes at small frequency *transfer*, $|\omega_1-\omega_4|\sim 0<\omega_0$ but that, nevertheless, involve electrons with high frequencies (ω_1 and ω_2). In a two-step RG analysis, the couplings $g_3(\omega_1,\omega_2,\omega_2,\omega_1)$, with different ω_1 and ω_2 are all indistinguishable since $|\omega_1-\omega_4|=0$ for all of them. Clearly, the two-step RG fails in this region.

It has been shown recently that the Luttinger charge exponent can be larger than one in the half filled one-dimensional Holstein-Hubbard model.[12] For the Luttinger liquid, the scalings of ground-state correlation functions are determined solely by the charge (K_ρ) and spin (K_σ) exponents. For example, in the spin-gapped regime, where $K_\sigma=0$, CDW and SC correlation functions scale as $O^{\text{CDW}}(x)\propto x^{-\alpha K_\rho}\equiv x^{-K_{\text{CDW}}}$, and $O^{\text{SC}}(x)\propto x^{-\beta/K_\rho}\equiv x^{-K_{\text{SC}}}$, with $\alpha=\beta=1$.[19–21] The dominant correlation is of CDW (SC) type for $K_\rho<1$ ($K_\rho>1$). This relation is not guaranteed to hold in the presence of phonons and retardation effects.[23] Moreover, using the Luttinger liquid theory to interpret the data from quantum Monte Carlo calculations for finite-size systems has to be performed with caution, in particular when the gap is vanishing exponentially with respect to the electron-phonon coupling.[6]

In conclusion, we have studied the ground state of 1DHHM at half filling using the MFRG method. This technique enables us to treat retardation effects from the phonons in a systematic way. We find SDW and CDW phases, and a direct transition between them. Analysis of the frequency dependence of the g_3 shows a shift in spectral weight indicating that the CDW instability near the transition is driven by dynamical umklapp processes. New phonon features are observed in Bechgaard salts at low temperatures[24–26] but their role is yet to be understood. The retardation effects and dynamical umklapp studied here may be relevant to the understanding of part of the rich phase diagram of the organics.

We thank Torsten Clay for instructive discussions. A.H.C.N. was supported through NSF Grant No. DMR-0343790.

[1] S.-W. Tsai, A. H. Castro Neto, R. Shankar, and D. K. Campbell, Phys. Rev. B **72**, 054531 (2005); Philos. Mag. **86**, 2631 (2006).
[2] T. Ishiguro and K. Yamaji, *Organic Superconductors* (Springer-Verlag, Berlin, 1990).
[3] *Conjugated Conducting Polymers*, edited by H. G. Weiss (Springer-Verlag, Berlin, 1992).
[4] O. Gunnarsson, Rev. Mod. Phys. **69**, 575 (1997).
[5] T. Holstein, Ann. Phys. (N.Y.) **8**, 325 (1959).
[6] J. E. Hirsch and E. Fradkin, Phys. Rev. B **27**, 4302 (1983); J. E. Hirsch, *ibid.* **31**, 6022 (1985).
[7] M. Fabrizio, C. Castellani, and C. Di Castro, Int. J. Mod. Phys. B **10**, 1439 (1996).
[8] C. Q. Wu, Q. F. Huang, and X. Sun, Phys. Rev. B **52**, R15683 (1995).
[9] E. Jeckelmann, C. Zhang, and S. R. White, Phys. Rev. B **60**, 7950 (1999).
[10] Y. Takada and A. Chatterjee, Phys. Rev. B **67**, 081102(R) (2003).
[11] Y. Takada, J. Phys. Soc. Jpn. **65**, 1544 (1996).
[12] R. T. Clay and R. P. Hardikar, Phys. Rev. Lett. **95**, 096401 (2005).
[13] M. Tezuka, R. Arita, and H. Aoki, Physica B **359**, 708 (2005); Phys. Rev. Lett. **95**, 226401 (2005).
[14] H. Fehske, G. Wellein, G. Hager, A. Weiße, and A. R. Bishop, Phys. Rev. B **69**, 165115 (2004).
[15] I. P. Bindloss, Phys. Rev. B **71**, 205113 (2005).
[16] R. Shankar, Rev. Mod. Phys. **66**, 129 (1994).
[17] K.-M. Tam, S.-W. Tsai, D. K. Campbell, and A. H. Castro Neto, arXiv:cond-mat/0603055 (unpublished).
[18] The interaction involves electrons with opposite or the same spins.
[19] V. J. Emery, in *Highly Conducting One-Dimensional Solids*, edited by J. T. Devreese, R. Evrand, and V. van Doren (Plenum, New York, 1979) p. 327.
[20] J. Sólyom, Adv. Phys. **28**, 201 (1979).
[21] J. Voit, Rep. Prog. Phys. **58**, 977 (1995).
[22] M. Nakamura, Phys. Rev. B **61**, 16377 (2000).
[23] D. Loss and T. Martin, Phys. Rev. B **50**, 12160 (1994).
[24] C. S. Jacobsen, D. B. Tanner, and K. Bechgaard, Phys. Rev. B **28**, 7019 (1983).
[25] D. Pedron, R. Bozio, M. Meneghetti, and C. Pecile, Phys. Rev. B **49**, 10893 (1994).
[26] N. Cao, T. Timusk, and K. Bechgaard, J. Phys. I **6**, 1719 (1996).